PCCP

Accepted Manuscript

ROYAL SOCIETY OF CHEMISTRY

www.rsc.org/pccp

Journal Name

ARTICLE

Sequential Energy and Electron Transfer in a Three-component System Aligned on a Clay Nanosheet

Received 00th January 20xx,
Accepted 00th January 20xx

DOI: 10.1039/x0xx00000x

www.rsc.org/

Takuya Fujimura[a, b], Elamparuthi Ramasamy[c], Yohei Ishida[d], Tetsuya Shimada[b,e], Shinsuke Takagi*[b,e], Vaidhyanathan Ramamurthy*[c]

To achieve the goal of energy transfer and subsequent electron transfer across three molecules, a phenomenon often utilized in artificial light harvesting systems, we have assembled a light absorber (that also serves as energy donor), an energy acceptor (that also serves as electron donor) and an electron acceptor on the surface of a anionic clay nanosheet. Since neutral organic molecules have no tendency to adsorb on the anionic surface of clay, positively charged water-soluble organic capsule was used to hold neutral light absorbers on the above surface. The three-component assembly was prepared by co-adsorption of cationic bipyridinium derivative, cationic zinc porphyrin and cationic octa amine encapsulated 2-acetylanthracene on exfoliated anionic clay surface in water. Energy and electron transfer phenomena were monitored by steady state fluorescence and picosecond time resolved fluorescence decay. Excitation of 2-acetylanthracene in the three component system resulted in energy transfer from 2-acethylanthracene to zinc porphyrin with 71% efficiency. Very little loss due to electron transfer from 2-acetylanthracene in cavitand to bipyridinium derivative was noticed. Energy transfer was followed by electron transfer from Zn-porphyrin derivative to cationic bipyridinium derivative with 81%. Analyses of fluorescence decays confirmed the occurrence of energy and subsequent electron transfer. Merging the concepts of supramolecular and surface chemistry we realized sequential energy and electron transfer between three hydrophobic molecules in water. Exfoliated transparent saponite clay served as a matrix to align the three photoactive molecules at close distance in aqueous solution.

Introduction

Photosynthesis, a process for survival, perfected by plants from the distinctive arrangement of pigments and other molecules on membrane surfaces collectively called the photosynthetic unit involves sequential physical (energy and electron transfer) and chemical events (oxidation and reduction) following absorption of light by the pigments.[1-9] Mimicking such a process (artificial photosynthesis) is an approach to solve the current energy crisis.[10-22] To achieve this goal one should be able to (a) organize donors and acceptors on a surface without aggregation and segregation, (b) transport energy to long distances through energy transfer (ET) process, (c) facilitate long distance electron transfer (eT), and (d) avoid unproductive side electron transfer from donor to acceptor. Such an assembly consisting of a minimum of three components should fulfil the condition outlined in Fig. 1[23-27] To achieve these controlled sequential energy transfer and electron transfer reaction in three component system, undesired electron transfer (*e.g.* between EnD and elA) should be supressed. Considering the intermolecular distance dependency of energy transfer reaction (it proceeds throw long distance by diploe

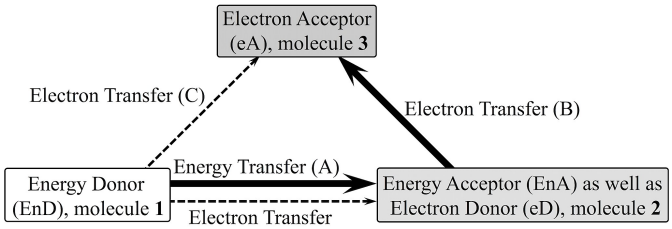

Fig. 1 Reaction flow in a three-component system.

[a] *Department of Physics and Materials Science, Interdisciplinary Graduate School of Science and Engineering, Shimane University, 1060 Nishi-kawatsu-cho, Matsue, Shimane 690-8504, Japan.*
[b] *Department of Applied Chemistry, Graduate School of Urban Environmental Sciences, Tokyo Metropolitan University, 1-1 Minami-osawa, Hachioji, Tokyo 192-0397, Japan. E-mail : takagi-shinsuke@tmu.ac.jp*
[c] *Department of Chemistry, University of Miami, Coral Gables, Florida 33146-0431, USA E-mail : murthy1@miami.edu*
[d] *Division of Material Science and Engineering, Faculty of Engineering, Hokkaido University, Kita 13, Nishi 8, Kita-ku, Sapporo, Hokkaido 060-8628, Japan.*
[e] *Center for Artificial Photosynthesis, Tokyo Metropolitan University, 1-1 Minami-ohsawa, Hachioji, Tokyo 192-0397, Japan.*

†Electronic Supplementary Information (ESI) available: Fig. S1-S5, calculation procedure for the energy transfer efficiency and the quenching efficiency in ($AA@OAm_2^{16+}$–$ZnTMPyP^{4+}$) ∩ clay system, calculation of Gibbs free energy change(ΔG_{el}) for the two electron transfer reaction, Stern-Volmer analysis of ($AA@OAm_2^{16+}$–$DNPV^{2+}$) ∩ clay system and ($ZnTMPyP^{4+}$–$DNPV^{2+}$) ∩ clay system, calculation procedure for efficiencies of the energy transfer, electron transfer and energy loss in three components system. See DOI: 10.1039/x0xx00000x

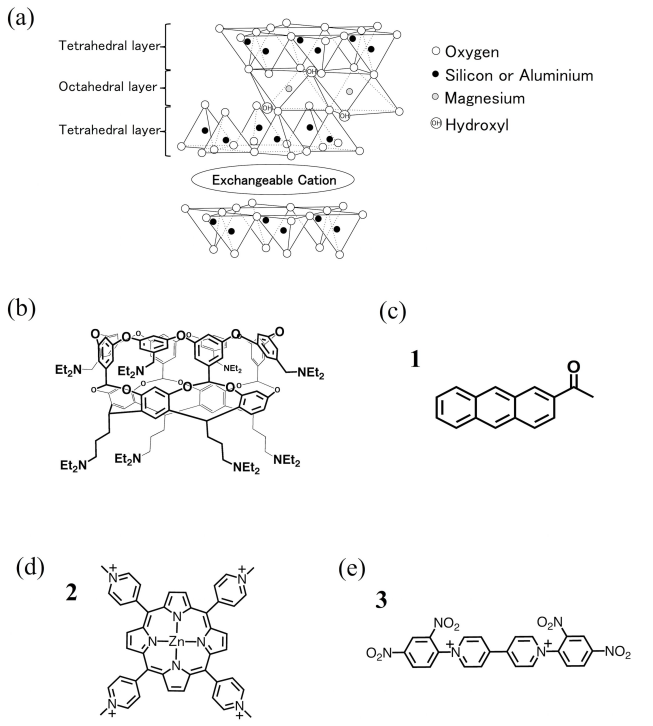

Fig. 2 Structure of (a) Saponite, (b) octa amine (OAm), (c) 2-acetylanthracene (AA), (d) tetrakis(1-methylpyridinium-4-yl)porphyrinato zinc ($ZnTMPyP^{4+}$), (e) 1,1'-bis(2,4-dinitrophenyl)-4,4'-bipyridinium ($DNPV^{2+}$).

interaction) and electron transfer reaction (it can't proceed throw long distance), electron transfer reaction between EnD encapsulated in cationic molecular capsule and cationic elA might supress because of the electric repulsion or steric effect. For the model study to establish the proof of principle, we have identified three molecules to serve as a light absorber (energy donor), energy acceptor (also serves as electron donor) and electron acceptor. With the help of clay surface and a cationic water-soluble cavitand, we have been able to organize these three molecules and establish the feasibility of light energy capture and transfer of energy and electron in an orderly manner. Structures of these three molecules, clay and cavitand are provided in Fig. 2.

Light absorber (energy donor), energy acceptor (that also serves as electron donor), and electron acceptor molecules were aligned on the surface of negatively charged saponite clay nanoparticles. The saponite clay when exfoliated into a single layer was transparent, 0.97 nm thick and had a particle size of *ca.* 50 nm.[28-31] The uniformly distributed anionic charges on the surface were separated by 1.2 nm. On these highly ordered anionic surfaces, cationic molecules could be assembled such that intercationic distance is ~1.2 nm.[28, 32] Of the three molecules presented in Fig. 2, the positively charged (tetrakis(1-methylpyridinium-4-yl)porphyrinato zinc ($ZnTMPyP^{4+}$) and 1,1'-bis(2,4-dinitrophenyl)-4,4'-bipyridinium ($DNPV^{2+}$) could be adsorbed on the surface of the saponite clay. As the neutral 2-acetylanthracene (AA) does not adsorb on the clay surface, the deep cavity cavitand, protonated octa amine (OAm; Fig. 2-(b)) capable of including various aromatic molecules by forming a capsule was used to place 2-acetylanthracene on the anionic clay surface along with $ZnTMPyP^{4+}$ and $DNPV^{2+}$. This supramolecular assembly made of two free cationic molecules, a host-guest cationic supramolecular assembly and an anionic clay surface utilized as an artificial light-harvesting model was investigated in the context of energy and electron transfer in aqueous solution.

The above described four-component assembly offers the following advantages: (a) aggregation of donor and acceptor molecules is avoided due to Columbic repulsion as OAm^{16+} capsule as well as $ZnTMPyP^{4+}$ and $DNPV^{2+}$ are cationic and (b) the assembly is held on the clay surface due to strong Coulombic attraction of cationic dyes $ZnTMPyP^{4+}$ and $DNPV^{2+}$ as well as cationic capsules (OAm^{16+} capsule) to the anionic clay surface. However due to lack of any specific interaction between OAm^{16+} capsules, $ZnTMPyP^{4+}$ and $DNPV^{2+}$ random distribution of the three molecules on the clay surface is expected. We had established earlier the possibility of energy and electron transfer between cavitand (octa acid) encapsulated donor and free acceptor in aqueous solution.[33–36] Recently we have demonstrated the energy transfer from donor $AA@OAm_2^{16+}$ (the symbol @ represents the inclusion of AA within OAm capsule) to $ZnTMPyP^{4+}$, both anchored on saponite clay surface.[37] In addition, we revealed that $guest@OAm_2^{16+}$ was using only 4 of the 16 cationic charges to adsorb on clay. It means that $guest@OAm_2^{16+}$ has excess free cationic charges, thus it is expected that electron transfer reaction between encapsulated guest and other naked cationic molecule could be suppressed by avoiding the collision of the molecules by electric repulsion. This consideration creates the expectation to suppress the undesired electron transfer reaction (Fig. 1, broken line). Energy and electron transfer phenomena were monitored by steady state fluorescence and picosecond time resolved fluorescence decay. Observations reported here establish the value of applying the principles of supramolecular chemistry while building artificial photosynthetic models.

EXPERIMENTAL

Materials

The synthetic saponite clay mineral used in this experiment was purchased from Kunimine Industries and used as such. The organic cavitand with amine functionality OAm was synthesized according to the reported procedure.[38] The guest molecules AA, $ZnTMPyP^{4+}$, and $DNPV^{2+}$ were purchased from Aldrich, Frontier Scientific and Tokyo Chemical Industry, respectively. They were used as received after ascertaining their purities by ^{1}H-NMR. Water was deionized with an ORGANO BB-5A system (PF filter × 2 + G-10 column).

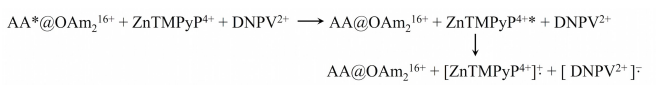

Fig. 3 Proposed reaction flow (energy transfer and subsequent electron transfer reaction) in present system.

The electronic absorption spectra were recorded with a Shimadzu UV-3150 spectrophotometer. Fluorescence spectra were monitored with an Edinburgh FS920CDT fluoroimeter equipped with a xenon lamp. TG/DTA measurements were carried out with a Shimadzu DTG-60H analyzer to determine the water content of materials. The time-resolved fluorescence measurement was conducted under photoncounting conditions (Hamamatsu Photonics, C4334 streak scope, connected with CHROMEX 250IS polychrometer) with an EKSPLA PG-432 optical parametric generator (430 nm, 25 ps fwhm, 20 μJ, 1 kHz) pumped by the third harmonic radiation of Nd^{3+} :YAG laser, EKSPLA PL2210JE (355 nm, 25 ps fwhm, 300 μJ, 1 kHz). The laser flux was reduced with neutral density filters to avoid multiphoton absorption processes and nonlinear effects.

Sample Preparation

Solution of OAm_2^{16+} and AA included in OAm_2^{16+} under acidic condition (pH = 1.0) were prepared by following the previously reported procedure.[34,37,38] Inclusion of AA within OAm_2^{16+} and the ratio of the host to guest complex were checked by ^{1}H NMR measurements and NMR titration experiments in water under acidic conditions (pH = 1.0). The stock solution of AA@OAm_2^{16+} was diluted with aqueous HCl to maintain a pH of 1.0. Guest molecules∩clay complex (thesymbol ∩ represents the adsorption of guests on the clay nanosheets.) was prepared by following the procedure described below.[34,37] Aqueous HCl solution and stock solutions of each guest molecule were added into a cuvette. The concentration of HCl aqueous solution was adjusted to keep the resulting dispersion at pH 1.0. The clay dispersion was added to the mixture with stirring to obtain a transparent complex dispersion. We had previously reported [34], adsorption of AA@OAm_2^{16+} on the clay surface without aggregation up to 400% cation exchange capacity (CEC). The fact that the capsule could be adsorbed to a maximum CEC of 400% indicated that AA@OAm_2^{16+} was using only 4 of the 16 cationic charges to adsorb on clay. Although AA@OAm_2^{16+} has 16 positive charges it behaves like a tetra-cationic porphyrin, with only the 4 cationic charges on the bottom of the AA@OAm_2^{16+} anchoring to the clay surface. In this article, 4 × [the number of AA@OAm_2^{16+}] is used to express the loading levels on the clay surface (% vs. CEC of the clay). Furthermore, we reported that guest@OAm_2^{16+} was using only 4 cationic charges (bottoms) of the 16 cationic charges to adsorb on clay, and the distances between each amino-groups of the OAm was shown in previous report.[34, 37] Considering these calculation and result, the inter-cationic distance of the OAm meets requirement of Size matching Effect. Since all cationic sites were utilized for adsorption by $ZnTMPyP^{4+}$ and $DNPV^{2+}$ the loading levels on the clay surface in these are expressed as follows: [the number of the $ZnTMPyP^{4+}$] × 4 and [the number of $DNPV^{2+}$] × 2 respectively. The loading levels of AA@OAm_2^{16+} and $ZnTMPyP^{4+}$ were set at 10%, to result in a 1:1 ratio of AA@OAm_2^{16+} and $ZnTMPyP^{4+}$. The loading level of $DNPV^{2+}$ was varied between 0 and 80%.

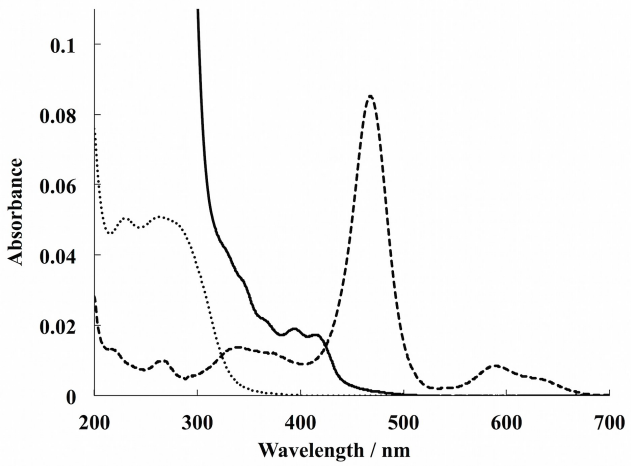

Fig. 4 Absorption spectra of AA@OAm_2^{16+}∩clay (solid line), $ZnTMPyP^{4+}$∩clay (broken line), and $DNPV^{2+}$∩clay (dotted line). Concentration of the AA@OAm_2^{16+}, $ZnTMPyP^{4+}$, $DNPV^{2+}$ and clay were set at 1.0 × 10^{-5} M (corresponding to 50% versus CEC of the clay), 5.0 × 10^{-7} M (corresponding to 2.5% versus CEC of the clay), 1.7 × 10^{-5} M (corresponding to 40% versus CEC of the clay) and 8.4 × 10^{-2} g L^{-1}, respectively.

Results and Discussion

Goal of the present study was to align three molecules on the surface of clay and establish the feasibility of light absorption and sequential energy transfer from molecule **1** to **2** and electron transfer from molecule **2** to **3** (Fig. 1). Thus in the three-component assembly light absorption by molecule **1** would ultimately result in the generation of radical ions at a site distant from the initial light absorption. For the system to be efficient like in photosystems the quenching of excited molecule **1** due to direct electron transfer from molecule **1** to molecule **2** or **3** in this assembly should be suppressed. The designed reaction flow in present system was shown in Fig. 3. Before embarking on a study of a three component supramolecular assembly, investigation and identification of the experimental conditions of excitation of molecule **1** (energy donor) in presence of molecules **2** and **3** and establishing the feasibility of energy transfer from **1** to **2** and electron transfer from **2** to **3** in a two component is crucial. In this study **1**, **2** and **3** are AA, $ZnTMPyP^{4+}$ and $DNPV^{2+}$. We thus begin the presentation with two-component system and proceed to three-component system.

Absorption spectra of AA@OAm_2^{16+}∩clay, $ZnTMPyP^{4+}$∩clay, $DNPV^{2+}$∩clay

Absorption spectra of AA@OAm_2^{16+}∩clay, $ZnTMPyP^{4+}$∩clay, and $DNPV^{2+}$∩clay are shown in Fig. 4. Experiments dealing with fluorescence quenching of AA and $ZnTMPyP^{4+}$ required selective excitation of the fluorophore in presence of quenchers.

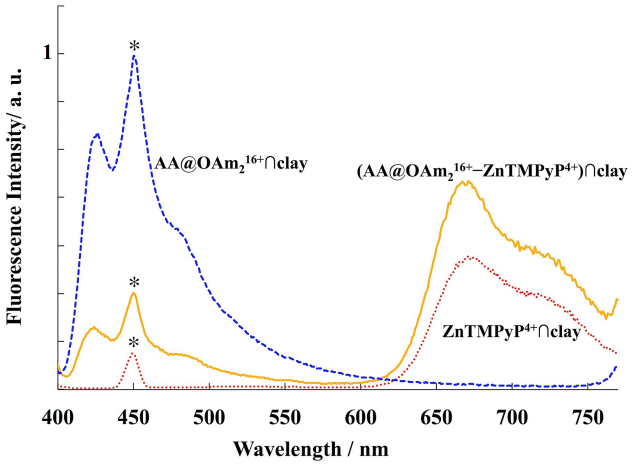

Fig. 5 Fluorescence spectra of AA@OAm_2^{16+}∩clay (blue broken line), $ZnTMPyP^{4+}$∩clay (red dotted line) and (AA@OAm_2^{16+}–$ZnTMPyP^{4+}$)∩clay (solid yellow line). Symbol ✻ denotes Raman scattering of incident light. Concentration of the AA@OAm_2^{16+}, $ZnTMPyP^{4+}$, and clay were set at 2.5×10^{-7} M (corresponding to 10% versus CEC of the clay), 2.5×10^{-7} M (corresponding to 10% versus CEC of the clay) and 1.0×10^{-2} g L^{-1}, respectively.

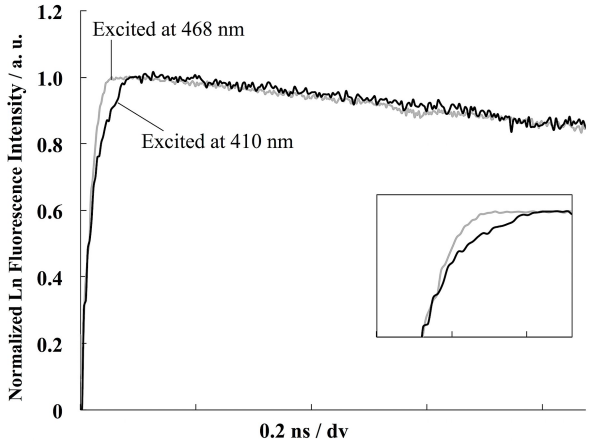

Fig. 6 Normalized time resolved fluorescence decays of (AA@OAm_2^{16+}–$ZnTMPyP^{4+}$)∩clay upon excitation at 410 nm (black line) and 468 nm (gray line). Inset: the enlarged Fig. around the peak top in Fig. 6. Concentration of the AA@OAm_2^{16+}, $ZnTMPyP^{4+}$ and clay were set at 5.0×10^{-6} M (corresponding to 10% versus CEC of the clay), 5.0×10^{-6} M (corresponding to 10% versus CEC of the clay) and 0.2 g L^{-1}, respectively.

This necessitated analysis of the absorption spectra of the three molecules AA, $ZnTMPyP^{4+}$ and $DNPV^{2+}$. It is important to note that both $ZnTMPyP^{4+}$ and AA@OAm_2^{16+} have overlapping absorption in the region 390 to 420 nm, and excitation in this region would result in the population of the excited states of both molecules requiring correction for the overlapping spectra when establishing energy transfer from AA@OAm_2^{16+} to $ZnTMPyP^{4+}$. $ZnTMPyP^{4+}$∩clay could be conveniently excited > 460 nm since it had distinct absorption above 460 nm and $DNPV^{2+}$∩clay had no absorption band over 380 nm. Recording the spectra at various loading levels made clear that the host-guest complex AA@OAm_2^{16+}, $ZnTMPyP^{4+}$ and $DNPV^{2+}$adsorbed on the clay surface did not aggregate even at loading levels up to 100, 100, 80% respectively.[28,34,39]

Energy transfer in two component (AA@OAm_2^{16+}–$ZnTMPyP^{4+}$)∩clay system

We previously reported energy transfer from excited AA@OAm_2^{16+} to $ZnMPyP^{4+}$ adsorbed on saponite clay surface at high loading levels.[36] To accommodate the third molecule ($DNPV^{2+}$) on an assembly of three different guest molecules on clay surface it was essential to establish the occurrence of energy transfer at low loading levels. Thus the loading levels of AA@OAm_2^{16+} and $ZnTMPyP^{4+}$ were set at 10% versus CEC of the clay. Fluorescence spectra with excitation wavelength set at 390 nm for AA@OAm_2^{16+}∩clay, $ZnTMPyP^{4+}$∩clay and co-adsorbed sample {(AA@OAm_2^{16+}–$ZnTMPyP^{4+}$)∩clay} are shown in Fig. 5. In the sample containing two components {(AA@OAm_2^{16+}–$ZnTMPyP^{4+}$)∩clay}, the fluorescence intensity of (AA@OAm_2^{16+}) decreased and that of ($ZnTMPyP^{4+}$) increased compared to those clay samples containing singlet component of either AA@OAm_2^{16+} or $ZnTMPyP^{4+}$. This suggested possible occurrence of energy transfer from excited AA@OAm_2^{16+} to $ZnTMPyP^{4+}$. Time resolved fluorescence measurements with excitation wavelengths set at 468 nm and 410 nm were carried out to confirm energy transfer from AA@OAm_2^{16+} to $ZnTMPyP^{4+}$ respectively (the former wavelength would excite both compounds while the latter would selectively excite $ZnTMPyP^{4+}$) and detected at 690-780 nm for fluorescence from $ZnTMPyP^{4+}$. The normalized fluorescence decays upon excitation at 468 nm and 410 nm are shown in Fig. 6. Also their fluorescence decay profiles, fitting curves and residual errors are provided as Fig. S1 in Supporting Information (SI). The decay curve obtained upon 468 nm excitation showed single exponential decay and fluorescence lifetime was determined to be 0.79 ns. On the other hand, when excitation wavelength was set at 410 nm a rise component was distinct. The observed emission was analyzed as a double-exponential decay with <0.10 ns rise and 0.79 ns decay. The difference in the two emission decay traces (468 and 410 nm excitation) supported our model that there is energy transfer from excited AA@OAm_2^{16+} to $ZnTMPyP^{4+}$ in the two component system.

Energy transfer efficiency was determined by the analysis of the fluorescence spectra according to the method outlined in SI.[39] The energy transfer efficiency (η_{ET}) and the quenching efficiency(φ_q), defined in equations 1 and 2, were determined to be 67% and 5%, respectively.

$$\eta_{ET} = \frac{k_{ET}}{k_{ET} + k_d^D + k_f^D + k_q} \quad (1)$$

$$\phi_q = \frac{k_q}{k_{ET} + k_d^D + k_f^D + k_q} \quad (2)$$

Energy transfer mechanism should be fluorescence resonance type considering the low absorbance of $ZnTMPyP^{4+}$ at experimental condition and the suppression of collision between donor and acceptor molecule by the encapsulation. Considering the distance dependence of fluorescence resonance energy transfer, the fact that the energy transfer proceeded distance is estimated to be 4.8 nm. We reported earlier that at high dye loading (average intermolecular distance is 2.4 nm) energy transfer rate constant from AA@OAm_2^{16+} to $ZnTMPyP^{4+}$ to be 1.9×10^9 s^{-1}.[35] Employing this rate constant,

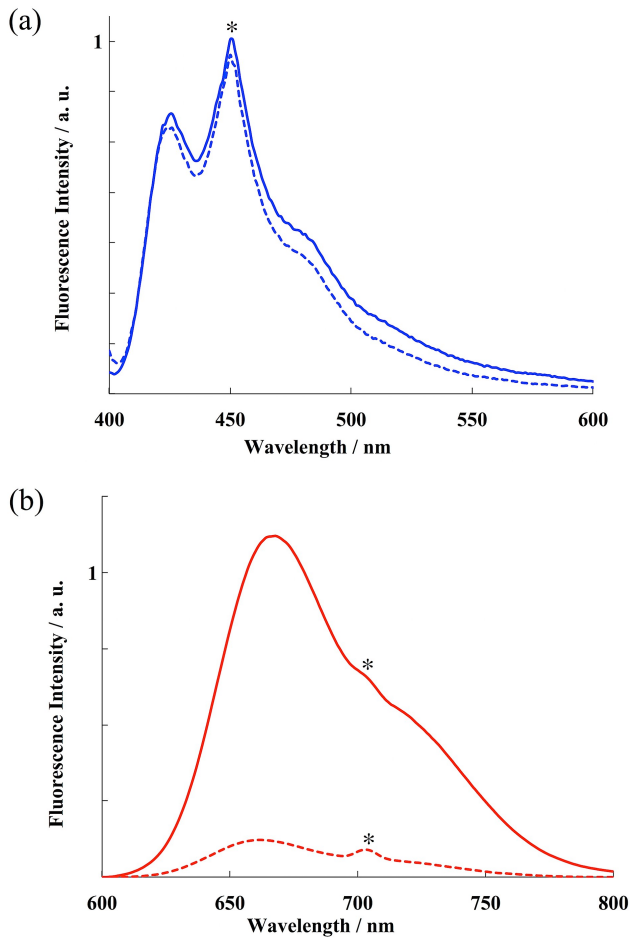

Fig. 7 (a) Fluorescence spectra of (AA@OAm_2^{16+}–$DNPV^{2+}$)∩clay (broken line) and AA@OAm_2^{16+}∩clay (solid line), (b) Fluorescence spectra of ($ZnTMPyP^{4+}$–$DNPV^{2+}$)∩clay (broken line) and $ZnTMPyP^{4+}$∩clay(solid line). The symbol * denotes Raman scattering of incident light. Concentration of the AA@OAm_2^{16+}, $ZnTMPyP^{4+}$, $DNPV^{2+}$ and clay were set at 2.5 × 10^{-7} M (corresponding to 10% versus CEC of the clay), 2.5 × 10^{-7} M (corresponding to 10% versus CEC of the clay), 4.0 × 10^{-6} M (corresponding to the 80% versus CEC of the clay) and 1.0 × 10^{-2} g L^{-1}, respectively.

the theoretical energy transfer rate constant and theoretical energy transfer efficiency at the current low loading level was calculated to be 2.9 × 10^7 s^{-1} and 0.27, respectively. Clearly the calculated efficiency is lower than the observed energy transfer efficiency. This suggests that the adsorbed dye molecules form island type of structure (Fig. S2 in SI) on the clay surfaces.

Electron transfer in two component systems: Electron transfer between AA@OAm_2^{16+} and $DNPV^{2+}$ and between $ZnTMPyP^{4+}$ and $DNPV^{2+}$

Having established the feasibility of energy transfer from AA@OAm_2^{16+} to $ZnTMPyP^{4+}$ we embarked on a study of electron transfer from $ZnTMPyP^{4+}$ to $DNPV^{2+}$ (B part in Fig. 1) and from AA@OAm_2^{16+} to $DNPV^{2+}$ (C part in Fig. 1). With the estimated exergonicity (Gibbs free energy (ΔG_{el}) as per the Rehm and Weller equation), exothermic electron transfer is expected in both systems (See SI for calculations).[39,41–43]

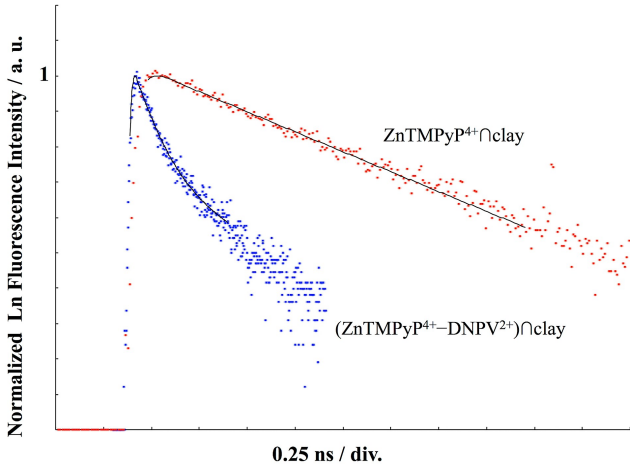

Fig. 8 Time resolved fluorescence decay curves of $ZnTMPyP^{4+}$∩clay (red dot) and ($ZnTMPyP^{4+}$–$DNPV^{2+}$)∩clay (blue dot). The black solid lines are fitting curves for those decay profiles. Concentration of the $ZnTMPyP^{4+}$, $DNPV^{2+}$ and clay were set at 5.0 × 10^{-6} M (corresponding to 10% versus CEC of the clay), 8.0 × 10^{-5} M (corresponding to 80% versus CEC of the clay) and 0.2 g L^{-1}, respectively.

The steady-state fluorescence spectra for AA@OAm_2^{16+}∩clay and $ZnTMPyP^{4+}$∩clay were recorded both in the presence and absence of $DNPV^{2+}$. The adsorption amount of $DNPV^{2+}$ was set at 80% versus CEC of the clay. As evident in Fig. 7(a), addition of $DNPV^{2+}$ had no effect on the fluorescence intensity of AA@OAm_2^{16+}∩clay. However, in the case of $ZnTMPyP^{4+}$∩clay addition of $DNPV^{2+}$ decreased the fluorescence (Fig. 7(b)). It indicated the occurrence of electron transfer reaction between $ZnTMPyP^{4+}$ to $DNPV^{2+}$. Another possibility of the fluorescence quenching of $ZnTMPyP^{4+}$ is the energy transfer from $ZnTMPyP^{4+}$ to $DNPV^{2+}$, but excitation energy of $ZnTMPyP^{4+}$ is lower than that of $DNPV^{2+}$, thus energy transfer process cannot proceed. These results are consistent with the conclusion that encapsulation of AA within OAm suppressed the electron transfer from AA* to $DNPV^{2+}$. Absence of electron transfer from AA*@OAm_2^{16+} to $DNPV^{2+}$ is experimentally convenient to study the electron transfer from $ZnTMPyP^{4+}$ to $DNPV^{2+}$ in presence of AA*@OAm_2^{16+}. The upward curvature (Fig. S3 in SI) of the Stern-Volmer plot prevented estimation of the electron transfer rate constant. Hence time-resolved fluorescence measurements were carried out both to confirm the dynamic nature of the fluorescence quenching and to estimate the electron transfer rate constant from excited $ZnTMPyP^{4+}$ to $DNPV^{2+}$. The time-resolved fluorescence decays of $ZnTMPyP^4$∩clay and ($ZnTMPyP^{4+}$–$DNPV^{2+}$)∩clay are reproduced in Fig. 8. For this experiment the adsorption amount of $DNPV^{2+}$ was set at 80% versus CEC of the clay. The emission from $ZnTMPyP^{4+}$∩clay exhibited a single exponential decay with 0.74 ns lifetime. On the other hand, emission from $ZnTMPyP^{4+}$ in presence of $DNPV^{2+}$ *i. e.*, [($ZnTMPyP^{4+}$–$DNPV^{2+}$)∩clay] decayed with two components having lifetimes 0.08 ns (77%) and 0.33 ns (23%). This suggested that the excited $ZnTMPyP^{4+}$ molecules that are quenched by $DNPV^{2+}$ are present in two environments (Fig. S4-(a) in SI).[38] Had all molecules been in the same environment

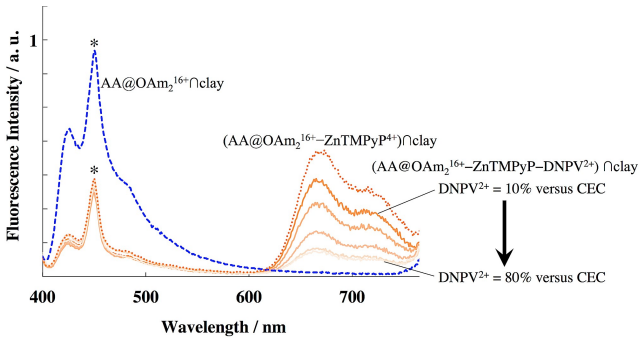

Fig. 9 Steady-state fluorescence spectra of AA@OAm_2^{16+}∩clay (broken blue line), (AA@OAm_2^{16+}–$ZnTMPyP^{4+}$)∩clay (dotted orange line) and (AA@OAm_2^{16+}–$ZnTMPyP^{4+}$– $DNPV^{2+}$)∩clay at each loading levels of $DNPV^{2+}$(solid orange lines). The symbol ✻ denotes Raman scattering of incident light. Excitation wavelength was set at 390 nm. Concentration of the AA@OAm_2^{16+}, $ZnTMPyP^{4+}$ and clay were set at 2.5×10^{-7} M (corresponding to 10% versus CEC of the clay), 2.5×10^{-7} M (corresponding to 10% versus CEC of the clay), and 1.0×10^{-2} g L^{-1}, respectively. Concentration of $DNPV^{2+}$ was changed from 0 to 4.0×10^{-6} M (corresponding to 0 and 80% versus CEC of the clay), respectively.

(Fig. S4-(b) in SI) a single exponential decay would be expected. The electron transfer rate constant was calculated by following equation.

$$k_{eT} = \frac{1}{\tau_i} - \frac{1}{\tau_0} \qquad (3)$$

where τ_0 is lifetime of the $ZnTMPyP^{4+}$∩clay and τ_i is lifetimes of the ($ZnTMPyP^{4+}$–$DNPV^{2+}$)∩clay. The electron transfer rate constants in the two environments were calculated to be 1.1×10^{10} s^{-1} and 1.7×10^{9} s^{-1}, respectively.

Energy Transfer and Subsequent Electron Transfer in Three Component System [AA@OAm_2^{16+}–$ZnTMPyP^{4+}$–$DNPV^{2+}$∩Clay]

In this three-component system, the goal is to probe the possibility of energy transfer from AA@OAm_2^{16+} to $ZnTMPyP^{4+}$ followed by electron transfer from the indirectly excited $ZnTMPyP^{4+}$ to $DNPV^{2+}$. To achieve this the fluorescence spectra of single component AA@OAm_2^{16+}∩clay, two component (AA@OAm_2^{16+}–$ZnTMPyP^{4+}$)∩clay (energy transfer system) and three component (AA@OAm_2^{16+}–$ZnTMPyP^{4+}$–$DNPV^{2+}$)∩clay (energy and subsequent electron transfer system) at various loading levels of $DNPV^{2+}$ were recorded with the excitation wavelength set at 390 nm (Fig. 9). The reduced fluorescence intensity of AA@OAm_2^{16+} in the two and three component systems compared to AA@OAm_2^{16+}∩clay is noticeable. With our earlier observation that $DNPV^{2+}$ does not quench the fluorescence of AA@OAm_2^{16+}, we interpret this fluorescence reduction as energy transfer from AA@OAm_2^{16+} to $ZnTMPyP^{4+}$. More importantly, the decreased fluorescence intensity in $ZnTMPyP^{4+}$ and AA's unchanged one with increased loading of $DNPV^{2+}$ is consistent with the conclusion of electron transfer from excited $ZnTMPyP^{4+}$ to $DNPV^{2+}$. In total these results suggest the occurrence of energy transfer and subsequent electron transfer in the three component

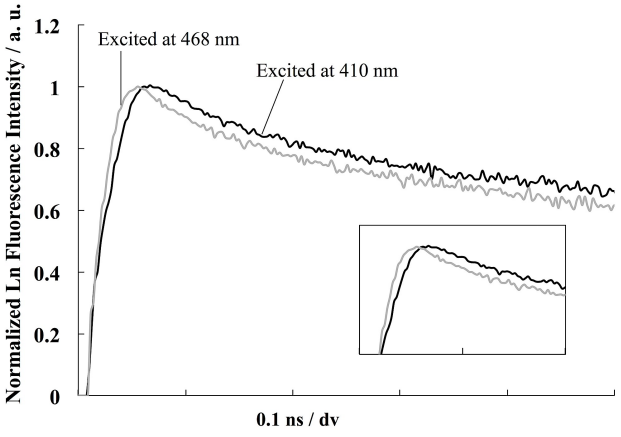

Fig. 10 Normalized time resolved fluorescence decay of (AA@OAm_2^{16+}–$ZnTMPyP^{4+}$–$DNPV^{2+}$)∩clay by excitation at 468 nm laser pulse (gray line) and at 410 nm laser pulse (black line). Inset: the enlarged Fig. around the peak of decay traces. Concentration of the AA@OAm_2^{16+}, $ZnTMPyP^{4+}$, $DNPV^{2+}$ and clay were set at 5.0×10^{-6} M (corresponding to 10% versus CEC of the clay), 5.0×10^{-6} M (corresponding to 10% versus CEC of the clay), 8.0×10^{-5} M (corresponding to 80% versus CEC of the clay) and 0.2 g L^{-1}, respectively.

Table 1. Efficiencies of energy transfer, electron transfer and energy loss in the three-component system.

Loading level of $DNPV^{2+}$ / % versus CEC of the clay	0	5	10	20	30	40	50	60	70	80
Energy transfer efficiency / %	67	68	72	72	73	72	73	73	72	70
Electron transfer efficiency / %	0	10	25	43	58	66	70	79	80	81
Energy loss efficiency / %	5	5	4	7	3	7	4	1	4	8

(AA@OAm_2^{16+}–$ZnTMPyP^{4+}$–$DNPV^{2+}$)∩clay system.

Further support for the above conclusion came from time resolved fluorescence studies of (AA@OAm_2^{16+}–$ZnTMPyP^{4+}$–$DNPV^{2+}$)∩clay. Normalized time resolved fluorescence decay of $ZnTMPyP^{4+}$ by exciting at 468 nm and 410 nm are shown in Fig. 10. Also their fluorescence decay profiles, fitting curves and residual errors are shown in Fig. S5. The decay fitted into a double exponential curve in a manner similar to the two component system {($ZnTMPyP^{4+}$–$DNPV^{2+}$)∩clay discussed above (Fig. 8) with life times of 0.04 ns (79%) and 0.30 ns (21%). These values are almost the same as the lifetime for $ZnTMPyP^{4+}$ in the two component ($ZnTMPyP^{4+}$-$DNPV^{2+}$)∩clay system (Fig. 8). The changes of the lifetimes should be ascribed to dyes' distribution change caused by presence of AA@OAm_2^{16+}, because electron transfers would be expected to be dependent on the distribution of the assembled dyes as described above. On the other hand, the observed delay in the emission when excitation wavelength was set at 410 nm indicates the presence of a rise component due to the population of excited $ZnTMPyP^{4+}$ through an energy transfer process. Then, the decay component is clearly fast compared to the decay in the absence of $DNPV^{2+}$. In the three components system the fluorescence decay could not be analyzed as double exponential, but could be analyzed tri-exponential curve composed of one rise component (<0.10 ns)

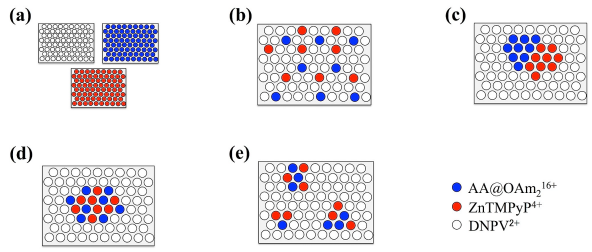

Fig. 11 Conceivable adsorption pattern of (AA@OAm$_2$$^{16+}$–ZnTMPyP^{4+}–DNPV^{2+})∩clay (a) Inter-sheet segregation, (b) Uniform, (c) Segregation, (d) Formation of the large island composed of AA@OAm$_2$$^{16+}$ and ZnTMPyP^{4+}, (e) Formation of small islands composed of AA@OAm$_2$$^{16+}$ and ZnTMPyP^{4+}.

and two decay components (0.05 ns and 0.33 ns). This rise component and fast decay components strongly indicates the occurrence of energy transfer and electron transfer reaction.

The efficiencies of energy transfer, energy loss and electron transfer at each DNPV^{2+} loadings could be estimated by analysis of the fluorescence spectra according to the method outlined in the Supporting Information. The efficiencies thus obtained are summarized in Table 1. From Table 1 the following conclusions could be drawn on the three-component system: (a) The energy transfer efficiency (71%) between AA@OAm$_2$$^{16+}$ and ZnTMPyP^{4+} was independent of the loading level of DNPV^{2+}. (b) The electron transfer efficiency between ZnTMPyP^{4+} and DNPV^{2+} increasing with increased loading level of the latter peaked at 81% when loading level of DNPV^{2+} is 80% versus CEC of the clay. (c) The average energy loss such as electron transfer reaction between AA@OAm$_2$$^{16+}$ and DNPV^{2+} was less than 5%. The data support the occurrence of both energy and electron transfer in this three component system, (AA@OAm$_2$$^{16+}$–ZnTMPyP^{4+}–DNPV^{2+})∩clay. The above energy and electron transfers would be expected to be dependent on the distribution of the three components AA@OAm$_2$$^{16+}$, ZnTMPyP^{4+} and DNPV^{2+} on the clay surface. The five types of distribution we visualize are shown in Fig. 11. Since the singlet-singlet energy transfer depends on inter molecular distance, efficient energy transfer is not expected in Fig. 11 (a) or (b). In the case of (c), energy transfer will proceed, but with low efficiency. In the pattern shown in Fig. 11 (d), and (e) energy and electron transfer are expected and the efficiency expected to be higher in the latter case because more number of electron donors (ZnTMPyP^{4+}) are surrounded by more number of electron acceptors (DNPV^{2+}). With the limited data on hand we can't draw conclusions regarding the distribution pattern of the three components on the clay surface. The fact that we are able to achieve electron transfer from a molecule that is indirectly excited by energy transfer suggest that most likely the distribution of the three components would follow pattern (e) shown in Fig. 11. We plan to probe the distribution using confocal fluorescence microscopy in the future.

Conclusions

We have demonstrated that it is possible to assemble three molecules in water with the help of a water-soluble organic cavitand and exfoliated single sheets of saponite clay. Selective excitation of one of them prompts sequential energy and electron transfer in which all three molecules participate. The energy and electron transfer efficiencies were estimated to be 71% and 81% respectively. There was few energy loss due to undesired electron transfer from the molecule that absorbed the light. Although this assembly is a long way from building an artificial photosynthetic apparatus, it established the value of combining strategies based on supramolecular and surface chemistry concepts. One of the problems in employing dyes (dye sensitized solar cells) to collect sunlight is they tend to aggregate. Organic capsules can arrest this process by enclosing them within itself and the clay surface can prevent aggregation by anchoring the ionic dyes through Columbic interactions. Results presented here open up new opportunities in developing new artificial light harvesting systems.

Acknowledgements

This work was partly supported by a Grant-in-Aid for Scientific Research on Innovative Areas "All Nippon Artificial Photosynthesis Project for Living Earth (AnApple)" grant (No. 25107521), a Grant-in-Aid for Scientific Research (B) (No. 24350100) from the JSPS and a Grant-in-Aid for JSPS Fellows (No. 2603441). YI thanks to Grant-in-Aid for Young Scientists from JSPS (14448322) and Sasakawa Scientific Research Grant from The Japan Science Society. VR is grateful to the National Science Foundation, USA (CHE-1411458) for financial support.

References

1. X. Hu, T. Ritz, A. Damjanović and K. Schulten, *J. Phys. Chem. B,* 1997, **101**, 3854-3871.
2. M. H. B. Stowell, T. M. McPhillips, D. C. Rees, S. M. Soltis, E. Abresch, and G. Feher. *Science,* 1997, **276**, 812-816.
3. L.-N. Liu and S. Scheuring, *Trends Plant Sci.,* 2013, **18**, 277-286.
4. A. Kuglstatter, U. Ermler, H. Michel, L. Baciou and G. Fritzsch, *Biochemistry,* 2001, **40**, 4253-4260.
5. J. Barber and B. Andersson, *Nature,* 1994, **370**, 31-34.
6. G. D. Scholes, G. R. Fleming, A. Olaya-Castro and R. van Grondelle, *Nat. Chem.,* 2011, **3**, 763-774.
7. A. N. Glazer, *Annu. Rev. Biochem.,* 1983, **52**, 125-157.
8. M. G. Müller, J. Niklas, W. Lubitz, and A. R. Holzwarth, *Biophys. J.,* 2003, **85**, 3899-3922.
9. J. Keating, G. Sankar, T. I. Hyde, S. Kohara and K. Ohara, *Phys. Chem. Chem. Phys.,* 2013, **15**, 8555-8565.
10. A. J. Bard and M. A. Fox, *Acc. Chem. Res.,* 1995, **28**, 141-145.
11. C. Y. Lee, O. K. Farha, B. J. Hong, A. A. Sarjeant, S. T. Nguyen and J. T. Hupp, *J. Am. Chem. Soc.,* 2011, **133**, 15858-15861.

12. R. Takahashi and Y. Kobuke, *J. Am. Chem. Soc.,* 2003, **125**, 2372-2373.
13. S. Funyu, T. Isobe, S. Takagi, D. A. Tryk and H. Inoue, *J. Am. Chem. Soc.,* 2003, **125**, 5734-5740.
14. B. Albinsson, and J. Martensson, *J. Photochem. Photobiol., C,* 2008, **9**, 138-155.
15. J. M. Smieja, E. E. Benson, B. Kumar, K. A. Grice, C. S. Seu, A. J. Miller, J. M. Mayer and C. P. Kubiak, *Proc. Natl. Acad. Sci. U. S. A.,* 2012, **109**, 15646-15650.
16. J. H. Alstrum-Acevedo and T. J. Meyer, *Inorg. Chem.,* 2005, **44**, 6802-6827.
17. H. Takeda, K. Koike, H. Inoue and O. Ishitani, *J. Am. Chem. Soc.,* 2008, **130**, 2023-2031.
18. H. Imahori, D. M. Guldi, K. Tamaki, Y. Yoshida, C. Luo, Y. Sakata and S. Fukuzumi, *J. Am. Chem. Soc.,* 2001, **123**, 6617-6628.
19. Y. Tachibana, L. Vayssieres and J. R. Durrant, *Nat. Photonics,* 2012, **6**, 511-518.
20. T. Yui, T. Kameyama, T. Sasaki, T. Torimoto and K. Takagi, *J. Porphyrins Phthalocyanines,* 2007, **11**, 428-433.
21. Y. Yamamoto, H. Takeda, T. Yui, Y. Ueda, K. Koike, S. Inagaki and O. Ishitani, *Chem. Sci.,* 2014, **5**, 639-648.
22. G. Leem, Z. A. Morseth, E. Puodziukynaite, J. Jiang, Z. Fang, A. T. Gilligan, J. R. Reynolds, J. M. Papanikolas and K. S. Schanze, *J. Phys. Chem. C*, 2014, **118**, 28535−28541.
23. J. Y. Liu, M. E. El-Khouly, S. Fukuzumi and D. K. Ng, *Chem. – Eur. J.,* 2011, **17**, 1605-1613.
24. F. D'Souza, P. M. Smith, M. E. Zandler, A. L. McCarty, M. Itou, Y. Araki and O. Ito, *J. Am. Chem. Soc.,* 2004, **126**, 7898-7907.
25. D. Gust, T. A. Moore and A. L. Moore, *Acc. Chem. Res.,* 1993, **26**, 198-205.
26. G. N. Lim, E. Maligaspe, M. E. Zandler and F. D'Souza, *Chem. – Eur. J.,* 2014, **20**, 17089-17099.
27. S. Fukuzumi, K. Saito, K. Ohkubo, T. Khoury, Y. Kashiwagi, M. A. Absalom, S. Gadde, F. D'Souza, Y. Araki, O. Ito and M. J. Crossley, *Chem. Commun.,* 2011, **47**, 7980-7982.
28. S. Takagi, T. Shimada, Y. Ishida, T. Fujimura, D. Masui, H. Tachibana, M. Eguchi and H. Inoue, *Langmuir,* 2013, **29**, 2108-2119.
29. M. Eguchi, H. Tachibana, S. Takagi, D. A. Tryk and H. Inoue, *Bul. Chem. Soc. Jpn.,* 2007, **80**, 1350-1356.
30. C. Bisio, G. Gatti, E. Boccaleri, L. Marchese, G. B. Superti, H. O. Pastore and M. Thommes, *Microporous and Mesoporous Mater.,* 2008, **107**, 90-101.
31. T. Shichi and K. Takagi, *J. Photochem. Photobiol., C,* 2000, **1**, 113–130.
32. S. Takagi, T. Shimada, M. Eguchi, T. Yui, H. Yoshida, D. A. Tryk and H. Inoue, *Langmuir,* 2002, **18**, 2265-2272.
33. E. Ramasamy, I. K. Deshapriya, R. Kulasekharan, C. V. Kumar and V. Ramamurthy, *Photochem. Photobiol. Sci.,* 2014, **13**, 301-309.
34. Y. Ishida, R. Kulasekharan, T. Shimada, S. Takagi and V. Ramamurthy, *Langmuir,* 2013, **29**, 1748-1753.
35. S. Gupta, A. Adhikari, A. K. Mandal, K. Bhattacharyya and V. Ramamurthy, *J. Phys. Chem. C,* 2011, **115**, 9593-9600.
36. M. Porel, A. Klimczak, M. Freitag, E. Galoppini and V. Ramamurthy, *Langmuir,* 2012, **28**, 3355–3359.
37. Y. Ishida, R. Kulasekharan, T. Shimada, V. Ramamurthy, and S. Takagi, *J. Phys. Chem. C,* 2014, **118**, 10198-10203.
38. R. Kulasekharan and V. Ramamurthy, *Org. Lett.,* 2011, **13**, 5092-5095.
39. S. Konno, T. Fujimura, Y. Otani, T. Shimada, H. Inoue and S. Takagi, *J. Phys. Chem. C,* 2014, **118**, 20504-20510.
40. Y. Ishida, T. Shimada, D. Masui, H. Tachibana, H. Inoue and S. Takagi, *J. Am. Chem. Soc.,* 2011, **133**, 14280-14286.
41. D. Rehm and A. Weller, *Isr. J. Chem.,* 1970, **8**, 259-271.
42. K. Kalyanasundaram and M. Neumann-Spallart, *J. Phys. Chem.,* 1982, **86**, 5163-5169.
43. S.-K. Lee, C.-M. Lim, J.-Y. Lee and D.-Y. Noh, *Bull. Korean Chem. Soc.,* 2011, **32**, 321-324.